

# An Efficient Solution to 3D Reconstruction from Two Uncalibrated Views under SV Constraint

Shuyang Dou<sup>1</sup>, Hiroshi Nagahashi<sup>2</sup> and Xiaolin Zhang<sup>3</sup>

<sup>1</sup>Department of Information Processing, Tokyo Institute of Technology,  
4259 Nagatsuta-cho, Midori-ku, Yokohama, Kanagawa 226-8503, Japan

<sup>2</sup>Imaging Science and Engineering Laboratory, Tokyo Institute of Technology,  
4259 Nagatsuta-cho, Midori-ku, Yokohama, Kanagawa 226-8503, Japan

<sup>3</sup>Precision and Intelligence Laboratory, Tokyo Institute of Technology,  
4259 Nagatsuta-cho, Midori-ku, Yokohama, Kanagawa 226-8503, Japan

Keywords: 3D Reconstruction, Uncalibrated Views, Focal Length Estimation, Standard Vergence.

Abstract: In this paper, an efficient solution is proposed to the problem of 3D reconstruction from two uncalibrated views under Standard Vergence (SV) constraint. This solution consists of three core steps: firstly, set up the camera configuration according to SV constraint; secondly, estimate camera's focal length and relative pose between two views; lastly, reconstruct the scene optimally by minimizing reprojection error. By analysing the degenerated camera motion under SV constraint, a novel method for efficiently estimating camera's focal length and relative pose is proposed. Both synthetic and real data experiments showed that this new method could provide close estimation, which resulted in fast convergence in the most time-consuming step of final optimization. The main contribution of this paper is that it is the first time to introduce SV constraint into 3D reconstruction problem, and an efficient solution which utilizes this constraint is proposed.

## 1 INTRODUCTION

Reconstructing the three dimensional (3D) model of scene has been a big challenge for many years in Computer Vision. A lot of methods for this problem were proposed. For example, Goesele et al. (2006) presented a robust multi-view stereo algorithm. Alexiadis et al. (2013) provided a real-time solution by using a multiple-Kinect capturing system. Besides, reconstruction from two uncalibrated views is an attracting approach. The reason for this is that only two views are used, neither prior camera calibration nor any knowledge about the scene is necessary. Thus, it is very cheap and easy to implement this method with just a camera.

In such an approach, camera needs to be automatically calibrated. This problem can be simplified to focal length estimation when semi-calibrated camera is used. This is a reasonable assumption for modern cameras. Many approaches of focal length estimation have been proposed during past years. Hartley (1992, in Kanatani et al., 2006) provided a solution by using the singular value decomposition (SVD) technique. Then, Pan et

al. (1995a, b, in Kanatani et al., 2006) proposed a new method by solving cubic equations. After that, Bougnoux (1998, in Kanatani et al., 2006) provided a closed form to estimate the focal length. Recently, Pernek and Hajder (2013) presented a novel solution by transforming this problem into the generalized eigenvalue problem introduced in Kukulova et al. (2008, in Pernek and Hajder, 2013). Besides, Stewenius et al. (2005) and Hartley and Li (2012) also proposed minimal approaches. Many methods will degenerate in *fixed configuration*, in which two optical axes intersect with each other. In order to deal with this difficulty, Brooks et al. (1998) and Kanatani and Matsunaga (2000) provided different solutions. However, these methods usually could only provide results with more deviations than traditional camera calibration methods, like the popular method proposed by Zhang (2000). As a result, reconstruction using these methods often converges slowly and lacks for accuracy.

In this paper, an efficient solution for 3D reconstruction from two uncalibrated views is presented by introducing an additional constraint on camera motion, called *Standard Vergence (SV)*

constraint. Under this constraint, the camera motion degenerates to a special planar case. Based on analyzing the geometric meaning of SV constraint, a new method is proposed for estimating camera's focal length and relative pose. Both synthetic and real data experimental results showed that this new method could provide very close estimations, and by using these initial values, a fast and accurate reconstruction solution could be achieved.

The following sections are organized like this: section 2 introduces fundamentals of SV constraint, section 3 explains the three core steps of our solution, section 4 shows the details of both synthetic and real data experiments, section 5 concludes the paper.

## 2 STANDARD VERGENCE FUNDAMENTALS

In order to explain the SV constraint more intuitively, a few useful terms will be described. Fig. 1 shows a fixed camera configuration. For each camera coordinate system, there are a *vertical axis* ( $Y$ -axis and  $Y'$ -axis for camera  $C$  and  $C'$  respectively) and a *horizontal plane* ( $XZ$ -plane and  $X'Z'$ -plane for  $C$  and  $C'$  respectively). Two optical axes,  $Z$ -axis and  $Z'$ -axis, intersect at point  $T$ , called the *optical intersection*. The angle  $\theta$  made by two optical axes is called the *convergence angle*. Furthermore, if the two distances from the optical intersection to each camera centre are same, then this case is called an *isosceles triangle configuration*.

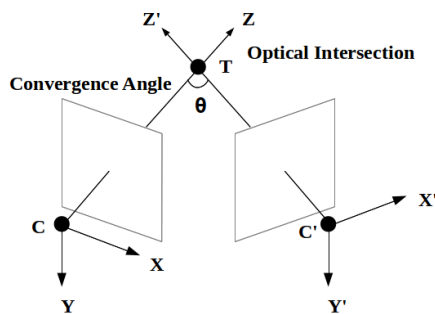


Figure 1: Fixed configuration.

SV constraint consists of two conditions: the first one is called *horizontal condition*, both of the two cameras share the same horizontal plane, which implies that there is no horizontal distortion between two views; the second one is called *intersection condition*, the two optical axes intersect with each

other, which is fair to say that it must be a fixed configuration. By using Fig. 1, the horizontal condition is equivalent to say that  $XZ$ -plane and  $X'Z'$ -plane must be the same plane, on the other hand, the intersection condition states that  $Z$ -axis and  $Z'$ -axis must intersect at some point  $T$ .

From these two conditions, the geometric meaning of SV constraint can be easily revealed as: the camera can only be moved and rotated on its horizontal plane. In this case, the camera motion degenerates to a special planar motion called *SV motion*.

SV motion was first proposed by Zhen et al. (2010). It originally comes from analysing the motion between two eyes of human beings. Each eye can be seen as a camera, thus, two eyes constitute a binocular system. It is easy to verify that the motion between two eyes obeys the intersection condition, because they are always focused on the target. Furthermore, the horizontal condition is also satisfied. If horizontal distortion exists between the two images captured by two eyes, the brain will be confused and unpleasant feeling will be felt.

Though SV motion is very familiar to us human beings, it is rarely used in 3D reconstruction problem. On the contrary, arbitrary or parallel binocular systems are currently much more widely used. This paper, for the first time, introduces SV constraint into 3D reconstruction problem. Because of the special degenerated form of camera motion under SV constraint, the problem becomes much simpler than general cases. Our new method for estimating camera's focal length and relative pose directly comes from this important observation.

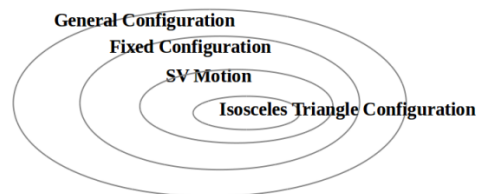


Figure 2: Different types of camera configuration.

Table 1: Applicable ranges for different focal length estimation methods.

| Method  | Applicable range  |
|---|---|
| General method, like (Bougnoux, 1998)                   | General configuration except fixed configuration            |
| Degenerated method, like (Kanatani and Matsunaga, 2000) | Fixed configuration except isosceles triangle configuration |
| New method proposed in this paper                       | SV motion   |

Many focal length estimation approaches, like (Bougnoux, 1998), will degenerate in fixed configuration, so they are not applicable to SV motion. Kanatani's method (Kanatani and Matsunaga, 2000) can handle the fixed configuration well. However, their method will degenerate in isosceles triangle case, which is a special case of SV motion. A new method is proposed in this paper which can handle all cases of SV motion. The applicable ranges for these methods are compared in Fig. 2 and Table 1.

### 3 PROPOSED SOLUTION

Three reasonable assumptions are necessary for the proposed solution: firstly, both of the two cameras are semi-calibrated, this is equivalent to say that except the focal length all the other intrinsic camera parameters are already known, this assumption is appropriate for modern cameras; secondly, the two cameras have similar or same focal length, which can be easily satisfied by moving one camera to different viewpoints without changing the zoom and focus values, or using a binocular system with two cameras of same series and synchronizing their zoom and focus values; lastly, the camera motion between two views must obey SV constraint.

According to the geometric meaning of SV, the camera configuration is easily set up to satisfy SV constraint like this: install the camera on a tripod and adjust it to be horizontal, then find a horizontal ground plane and place the equipment on it. The motion, which is composed by translating and rotating this equipment freely on the ground without changing the tripod's height, as well as camera's zoom and focus value, is SV motion. Thus, with a camera, a tripod and a horizontal ground plane, SV motion can be easily achieved manually.

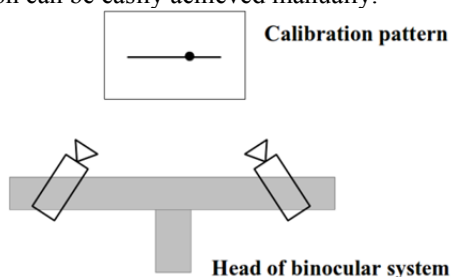


Figure 3: Calibration of binocular system.

For the case of using a binocular system, SV motion can be achieved by calibrating the position of each camera. In Fig. 3, a simple calibration

pattern of a line and an arbitrary marked point on it is used. Each camera is adjusted accordingly so that the projection of the marked point is located at the image centre, and the projection of the line is parallel to the image's horizontal axis. Finally, the camera motion becomes a SV motion. Note that, after this calibration step, each camera can only be rotated about its vertical axis. However, the head of the binocular system can be freely moved.

It is more challenging to satisfy SV constraint for a fully active binocular system, in which each camera can be moved freely. The basic idea is analysing and eliminating the horizontal distortion between two views. However, no details about such algorithm will be discussed in this paper.

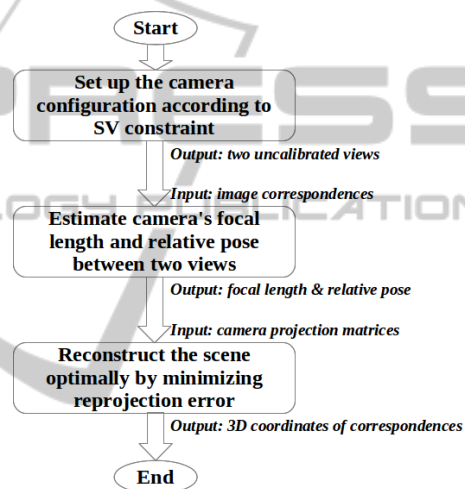


Figure 4: Flow chart of proposed solution.

The flow chart of proposed solution is showed in Fig. 4. It consists of three core steps: firstly, set up the camera configuration according to SV constraint, the method described previously is implemented in this step; secondly, estimate camera's focal length and relative pose between two views, this is done by using a new method which will be explained in detail later; lastly, reconstruct the scene optimally by minimizing reprojection error, this step can be sequentially divided into two stages: at first, a quick linear reconstruction is given by using the triangulation method; then, the reconstruction is refined by a non-linear optimization step using sparse Levenberg-Marquardt (LM) method (Hartley and Zisserman, 2004: 602). There are other works, like matching correspondences between the first and second step, need to be done in this solution. However, no discussion on these will be developed here because they are not focus points of this paper.

The new method for estimating camera's focal

length and relative pose used in step 2 is directly deduced by utilizing the degenerated form of camera motion. Usually, a  $3 \times 3$  orthogonal matrix  $R$  and a 3-element vector  $t$  are used to parameterize the camera's relative pose. In SV motion, camera only rotates about its vertical axis, so only one parameter, the convergence angle, is sufficient to describe the rotation. Thus, the degree of freedom (DOF) of  $R$  is reduced from 3 to 1. Meanwhile, the translation only happens on camera's horizontal plane, so the translation element of  $t$  along the vertical optical axis is zero. Thus, vector  $t$  has DOF of 2. As a result, under SV motion, matrix  $R$  and vector  $t$  will degenerate to the following forms:

$$R = \begin{bmatrix} \cos\theta & 0 & -\sin\theta \\ 0 & 1 & 0 \\ \sin\theta & 0 & \cos\theta \end{bmatrix} \quad (1)$$

$$t = \begin{bmatrix} t_x \\ 0 \\ t_z \end{bmatrix} \quad (2)$$

where  $\theta$  represents the convergence angle.

The essential matrix will have a special degenerated form as shown in eq. (3) by substituting eq. (1) and (2) into its decomposition form.

Now, by using eq. (3), the relationship between the fundamental and essential matrices provided by Hartley and Zisserman (2004: 257) can be developed as eq. (4), where  $K$  and  $K'$  are camera calibration matrices, with same unknown focal length value  $f$  and known principle point located at  $(u_1, v_1)$ ,  $(u_2, v_2)$  respectively.

$$\begin{aligned} E &= [t]_{\times} R = \begin{bmatrix} 0 & -t_z & 0 \\ t_z & 0 & -t_x \\ 0 & t_x & 0 \end{bmatrix} \begin{bmatrix} \cos\theta & 0 & -\sin\theta \\ 0 & 1 & 0 \\ \sin\theta & 0 & \cos\theta \end{bmatrix} \\ &= \begin{bmatrix} 0 & -t_z & 0 \\ t_z \cos\theta + t_x \sin\theta & 0 & -t_z \\ 0 & t_x & 0 \end{bmatrix} \\ &= \begin{bmatrix} 0 & e_{12} & 0 \\ e_{21} & 0 & e_{23} \\ 0 & e_{32} & 0 \end{bmatrix} \end{aligned} \quad (3)$$

The fundamental matrix can be directly estimated from correspondences. Thus, from eq. (3) and (4), it is easy to deduce eq. (5) to (9), which give a solution to  $R$ ,  $t$  and  $f$ .

$$\cos\theta = -\frac{f_{12}^2 u_2 + f_{21}^2 u_1 + f_{12} f_{32} + f_{21} f_{23}}{f_{12} f_{21} u_1 + f_{12} f_{21} u_2 + f_{12} f_{23} + f_{21} f_{32}} \quad (5)$$

$$\sin\theta = \sqrt{1 - \cos^2\theta} \quad (6)$$

$$t_x = \frac{f_{21} + f_{12} \cos\theta}{\sin\theta} \quad (7)$$

$$t_z = -f_{12} \quad (8)$$

$$f = \frac{f_{23} + f_{21} u_1}{t_z \sin\theta - t_x \cos\theta} \quad (9)$$

From eq. (7) to (9), it is easy to see that this method will degenerate only when  $\theta$  is zero. In this case, two optical axes will be parallel to each other. This is an obvious violation of the intersection condition of SV constraint. So, under SV constraint, this method can always give a solution. However, due to image noises, mismatching of correspondences or other reasons,  $\cos\theta$  may be greater than 1, and consequently  $\sin\theta$  will take imaginary value, in which case this method will fail.

Thus, it can be concluded that this method is applicable to any SV motion, though sometimes imaginary result might be given due to noises or other reasons.

## 4 EXPERIMENTS

### 4.1 Comparison Experiment

The goal for this experiment is to compare the efficiency of our new method with Kanatani's method (Kanatani and Matsunaga, 2000) on task of focal length estimation. The source code of their method is provided by Yamada et al. (2009). Totally 211 3D points from a part of a sphere surface, generated by ParaView (Kitware Inc. et al., 2013), are projected to each image plane (Fig. 5). The position and orientation of each camera are adjusted by two parameters as shown in Fig. 6: the convergence angle  $\theta$  and the distance ratio  $dr$ . It is easy to verify that each pair of  $\theta$  and  $dr$  can uniquely define a triangle  $\Delta CTC'$  up to scale. Thus, any SV motion can be achieved by setting proper values for  $\theta$  and  $dr$ .

$$\begin{aligned} F &= K'^T E K^{-1} = \begin{bmatrix} 1 & 0 & 0 \\ 0 & 1 & 0 \\ -u_2 & -v_2 & f \end{bmatrix} \begin{bmatrix} 0 & e_{12} & 0 \\ e_{21} & 0 & e_{23} \\ 0 & -e_{32} & 0 \end{bmatrix} \begin{bmatrix} 1 & 0 & -u_1 \\ 0 & 1 & -v_1 \\ 0 & 0 & f \end{bmatrix} \\ &= \begin{bmatrix} 0 & e_{12} & -e_{12} v_1 \\ e_{21} & 0 & -e_{21} u_1 + e_{23} f \\ -e_{21} v_2 - e_{12} u_2 + e_{32} f & e_{21} u_1 v_2 - e_{23} f v_2 + e_{12} u_2 v_1 - e_{32} f v_1 & 0 \end{bmatrix} = \begin{bmatrix} f_{11} & f_{12} & f_{13} \\ f_{21} & f_{22} & f_{23} \\ f_{31} & f_{32} & f_{33} \end{bmatrix} \end{aligned} \quad (4)$$

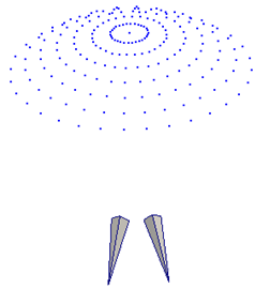


Figure 5: 3D points and cameras.

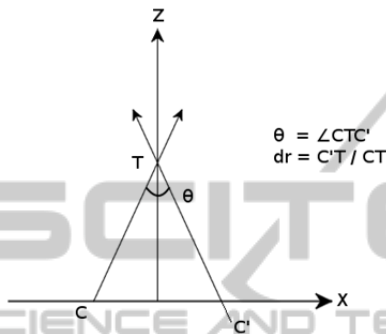


Figure 6: Camera configuration parameters.

In this experiment, the convergence angle  $\theta$  was chose from  $10^\circ$  to  $100^\circ$  with step of  $20^\circ$ . The distance ratio  $dr$  was chose from 0.5 to 1.5 with step of 0.1. The value 1.0 was skipped, because this is an isosceles configuration, in which case Kanatani's method (Kanatani and Matsunaga, 2000) will degenerate.

The true focal length was  $\bar{f} = 1000$  pixels for both cameras. A Gaussian noise with standard derivation  $\sigma = 0.5$  pixels was added to each image. Each configuration was tested 1000 times. The Root Mean Squares (RMS) error, which is defined as eq. (10), and computation time for each method is given in Fig. 7 to 10.

$$E_{RMS} = \sqrt{\frac{1}{1000} \sum_{i=1}^{1000} (f_i - \bar{f})^2} \quad (10)$$

The average RMS error for our method was about 14.8999 pixels, while 302.1656 pixels for Kanatani's method (Kanatani and Matsunaga, 2000). The reason for this is that only the intersection condition is used in their method, while the horizontal condition is also considered in our method. In other words, our method is only valid for SV motion, a much more specified applicable range than their method. It is common that a solution to a highly specified problem gain more accuracy than a solution to a more general problem.

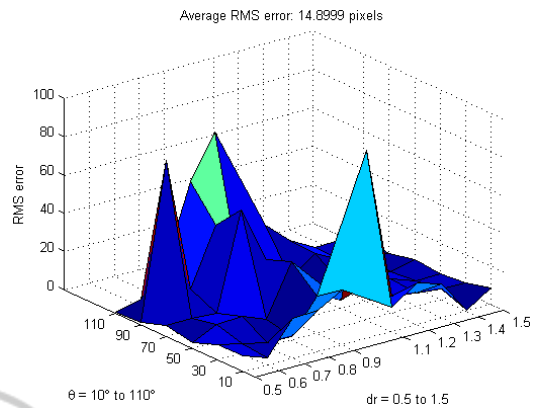


Figure 7: RMS error of our method.

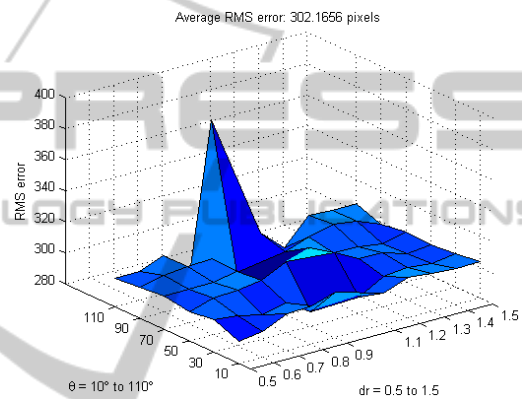


Figure 8: RMS error of Kanatani's method.

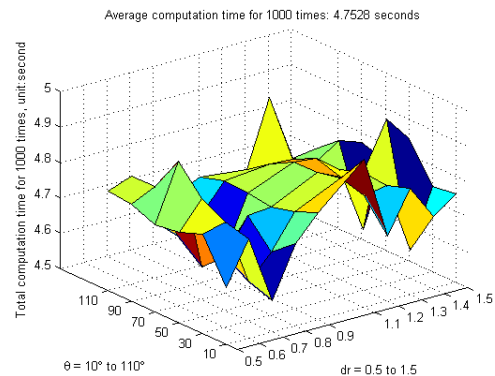


Figure 9: Computation time of our method.

The average computation time for 1000 times was 4.7528 seconds and 75.1425 seconds for our method and Kanatani's method (Kanatani and Matsunaga, 2000) respectively. The reason for significant shortening of computation time is simple: it only takes a few elementary calculations in our method, while polynomial calculations are necessary in their method.

In a conclusion, this experiment showed that



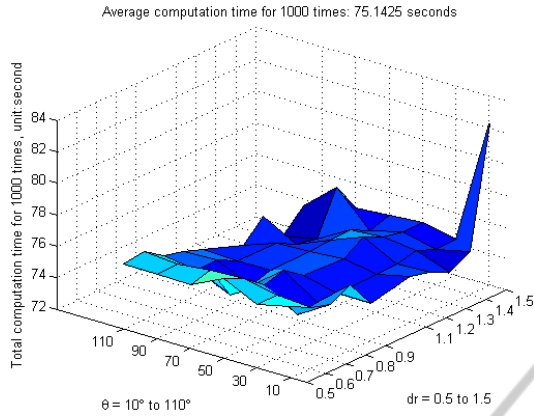


Figure 10: Computation time of Kanatani's method.

under SV constraint, our method is much more efficient than Kanatani's method (Kanatani and Matsunaga, 2000) for the task of focal length estimation.

#### 4.2 Real Scene Images Experiment

In this experiment, the efficiency of the proposed solution for 3D reconstruction was test by using both outdoor and indoor scene images. The camera configuration method described in section 3 was implemented. Totally 124 and 75 image correspondences, for outdoor and indoor scenes respectively, were selected manually, which were considered to represent the geometric shape of the scene well. Then, the 3D coordinate for each coordinate was reconstructed by using the proposed solution. Accuracy is represented by the RMS reprojection error, which is defined as eq. (11), where  $(x_i, y_i)$  and  $(x'_i, y'_i)$  are reprojected image points,  $(\tilde{x}_i, \tilde{y}_i)$  and  $(\tilde{x}'_i, \tilde{y}'_i)$  are manually selected image points.

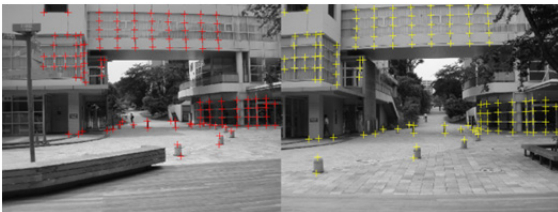


Figure 11: Manually selected correspondences (outdoor).



Figure 12: Two views of 3D points (outdoor).

Table 2: Optimization results (outdoor): reprojection error and focal length estimation, units for all values are pixel.

|  |                                      |
|--|--------------------------------------|
| RMS reprojection error                         | 1st loop: 7.1573<br>2nd loop: 0.5174 |
| Initial focal length estimation ( $f_u, f_v$ ) | (1322.6, 1322.6)                     |
| Optimal focal length of 1st camera             | (1322.5, 1322.8)                     |
| Optimal focal length of 2nd camera             | (1180.9, 1319.3)                     |

From Fig. 11 and 12, it can be easily confirmed that the reconstructed shape of the building is consistent to its real geometric shape. In Fig. 14, the reconstructed two orthogonal faces of the magic cube, and the curved surface of the cup represent the shape of the objects well.

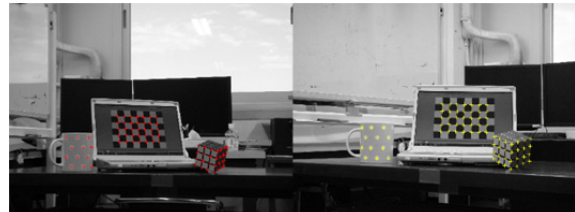


Figure 13: Manually selected correspondences (indoor).

$$E_{RMS} = \sqrt{\frac{1}{248} \sum_{i=1}^{124} ((x_i - \tilde{x}_i)^2 + (y_i - \tilde{y}_i)^2 + (x'_i - \tilde{x}'_i)^2 + (y'_i - \tilde{y}'_i)^2)} \quad (11)$$



Figure 14: Two views of 3D points (indoor).

Table 3: Optimization results (indoor): reprojection error and focal length estimation, units for all values are pixel.

|  |   |
|--|---|
| RMS reprojection error                         | 1st loop: 59.5622<br>2nd loop: 1.4326<br>3rd loop: 0.5576 |
| Initial focal length estimation ( $f_u, f_v$ ) | (3613.5, 3613.5)  |
| Optimal focal length of 1st camera             | (3620.6, 3652.6)  |
| Optimal focal length of 2nd camera             | (3646.6, 3410.2)  |

From the data showed in Table 2 and 3, it can be known that the final reconstruction result is reasonably high accurate, whose RMS reprojection error is about 0.5 pixels. Meanwhile, the non-linear optimization step converged very fast, which only used 2 and 3 iterations for outdoor and indoor scenes respectively. One of the reasons for this fast convergence is highly accurate initial estimation for focal length provided by our method.

For conclusion, both for outdoor and for indoor environments, the new method can provide a close estimation of focal length, which can dramatically facilitate the most time-consuming optimization step of 3D reconstruction.

## 5 CONCLUSIONS

In this paper, a special planar camera motion, called SV motion, is introduced to the problem of 3D reconstruction from two uncalibrated views. An efficient solution to this problem is proposed. This solution uses a new method for estimating camera's focal length and relative pose. Both synthetic and

real data tests showed that this method could provide close initial values. As a result, the non-linear optimization, which is the most time-consuming step of 3D reconstruction, could converge very fast. In a conclusion, an efficient solution is achieved to the problem of 3D reconstruction from two uncalibrated views under Standard Vergence (SV) constraint.

The main contribution of this paper is that it is the first time to introduce SV constraint into 3D reconstruction problem, and an efficient solution which utilizes this constraint is proposed.

## REFERENCES

- Alexiadis, D. S., Zarpalas, D. and Daras, P. (2013) Real-time, full 3-D reconstruction of moving foreground objects from multiple consumer depth cameras. *IEEE Trans. Multimedia*. 15(2):339-358.
- Bougnoux, S. (1998) From projective to Euclidean space under any practical situation, a criticism of self-calibration. In: *Proc. 6th Int. Conf. Comput. Vision*, Bombay, India, 790-796.
- Brooks, M. J., de Agapio, L., Huynh, D. Q. and Baumela, L. (1998) Towards robust metric reconstruction via a dynamic uncalibrated stereo head. *Image Vision Comput.* 16(14):989-1002.
- Goesele, M., Curless, B. and Seitz, S. M. (2006) Multi-view stereo revisited. In: *Proc. 2006 IEEE Comput. Society Conf. Comput. Vision Pattern Recog.* New York, NY, USA. 2:2403-2409.
- Hartley, R. I. (1992) Estimation of relative camera positions for uncalibrated cameras. In: *Proc. 2nd Euro. Conf. Comput. Vision*, Santa Margherita Ligure, Italy, 579-587.
- Hartley, R. and Zisserman, A. (2004) *Multiple view geometry in computer vision*. 2nd ed. Cambridge: Cambridge University Press.
- Hartley, R. and Li H. (2012) An efficient hidden variable approach to minimal-cal camera motion estimation. *IEEE Trans. Pattern Anal. Mach. Intell.* 34(12):2303-2314.
- Kanatani, K. and Matsunaga, C. (2000) Closed-form expression for focal lengths from the fundamental matrix. In: *Proc. 4th Asian Conf. Comput. Vision*, Taipei, Taiwan, 1:128-133.
- Kanatani, K., Nakatsuji, A. and Sugaya, Y. (2006) Stabilizing the focal length computation for 3-D reconstruction from two uncalibrated views. *Int. J. Comput. Vision*. 66(2):109-122.
- Kitware Inc., Sandia National Laboratories and Computational Simulation Software, LLC. (2013) *ParaView* (Version 4.0.1) [Computer program]. Available from <http://www.paraview.org> [Accessed 22 Jul. 2013].
- Kukelova, Z., Bujnak, M. and Pajdla, T. (2008) Polynomial eigenvalue solutions to the 5-pt and 6-pt

- relative pose problems. In: *Proc. British Machine Vision Conf.* Leeds, UK, 565-574.
- Pan, H.-P., Brooks, M. J. and Newsam, G. N. (1995a) Image resituation: initial theory. In: *Proc. SPIE: Videometrics IV*, Philadelphia, PA, USA, 2598:162-173.
- Pan, H.-P., Huynh, D. Q. and Hamlyn, G. K. (1995b) Two-image resituation: practical algorithm. In: *Proc. SPIE: Videometrics IV*, Philadelphia, PA, USA, 2598:174-190.
- Pernek, A. and Hajder, L. (2013) Automatic focal length estimation as an eigenvalue problem. *Pattern Recogn. Lett.* 24(9):1108-1117.
- Stewenius, H., Nister, D., Kahl, F. and Schaffalitzky, F. (2005) A minimal solution for relative pose with unknown focal length. In: *Proc. 2005 IEEE Comput. Society Conf. Comput. Vision Pattern Recog.* San Diego, CA, USA, 2:789-794.
- Yamada, K., Kanazawa, Y., Kanatani, K. and Sugaya, Y. (2009) *3DRec-MATLAB* [Computer Program]. Available from: <http://www.img.cs.tut.ac.jp/programs/index.html> [Accessed 22 Jul. 2013].
- Zhang, Z. (2000) A flexible new technique for camera calibration. *IEEE Trans. Pattern Anal. Mach. Intell.* 22(11):1330-1334.
- Zhen, Z., Miao, Y., Sato, M. and Zhang, X. (2010) Automatic 3D photographing device, In: *Proc. ASIAGRAPH*, Tokyo, Japan, 4(1):235-237.

WILEY  
PRESS  
TECHNOLOGY PUBLICATIONS